

Field-doping of C_{60} crystals: Polarization and Stark splitting

Samuel Wehrli,^{1,*} Erik Koch,² and Manfred Sigrist¹

¹*Theoretische Physik, ETH-Hönggerberg, CH-8093 Zürich, Switzerland*

²*Max-Planck-Institut für Festkörperforschung, Heisenbergstraße 1, 70569 Stuttgart, Germany*

(Dated: November 2, 2018)

We investigate the possibility of doping C_{60} crystals by applying a strong electric field. For an accurate description of a C_{60} field-effect device we introduce a multipole expansion of the field, the response of the C_{60} molecules, and the Stark splitting of the molecular levels. The relevant response coefficients and splittings are calculated *ab initio* for several high symmetry orientations. Using a group theoretic analysis we extend these results to arbitrary orientations of the C_{60} molecules with respect to the external field. We find that, surprisingly, for the highest occupied (HOMO) and the lowest unoccupied molecular orbital (LUMO), respectively, the two leading multipole components lift the degeneracy of the molecular level in the same way. Moreover the relative signs of the splittings turn out to be such that the splittings add up when the external field induces charge into the respective level. That means that when charge carriers are put into a level, its electronic structure is strongly modified. Therefore, in general, in C_{60} field-effect devices charge is not simply put into otherwise unchanged bands, so already because of this their physics should be quite different from that of the alkali-doped fullerenes.

PACS numbers: 73.61.Wp, 73.90.+f, 74.70.Wz

I. MOTIVATION

The proposal of doping C_{60} crystals in a field-effect device (FET) and the possibility of metallic conduction and even superconductivity in such devices had raised widespread interest. While the revelation of dishonest data handling in some cases¹ led to a severe damping of the initial enthusiasm, fundamental aspects of field effect doping remains a timely and interesting problem. For field-effect transistors made with self-assembled monolayers this question was addressed in Ref. 2 and for the reported enhancement of the superconducting transition temperature in C_{60} crystals intercalated with haloform molecules in Refs. 3. Attempts to observe the field-effect in graphite were reported in Ref. 4. Here we address, from a theoretical point of view, the question how strongly C_{60} can be doped in an electric field before its electronic structure is substantially changed and how this structure changes in even stronger fields. This is relevant for understanding the fundamental features of field-effect devices based on C_{60} and involves a number of interesting physical problems.

It appears that doping C_{60} crystals in a field-effect device (FET) is very hard to achieve in practice, one of the reasons being the exceptionally strong fields that are required. Very strong fields, however, not only induce charge carriers, but also polarize the molecules, and, due to the Stark effect, in general, lift degeneracies. These effects are of particular importance, as C_{60} is quite polarizable, and as its molecular levels are highly degenerate. The term “field-doping” naively implies that these effects are small, such that the main effect of the external field is inducing charge carriers into electronic levels which are essentially unaffected by the field. It is clear that if the external field is strong enough, the electronic structure of the crystal will be strongly modified by the field, and

one thus can no longer speak of doping. A fundamental question about field-effect devices is therefore connected with the doping levels achievable, before the electronic structure of the active material is substantially altered. Moreover we discuss in detail how the electronic structure is changed, when the external field is beyond this “doping limit”. In this regime the commonly used analogy of the field-doped C_{60} with the alkali-doped fullerenes no longer holds. Nevertheless a field-effect device with high carrier concentration would be an interesting device in its own right. One might, e.g., speculate that for C_{60} in a strong electric field the electron-phonon coupling is enhanced compared to unperturbed C_{60} , as for molecular orbitals of lower symmetry less couplings are forbidden by symmetry.

For a first estimate of the fields involved in field-doping, consider a simple capacitor. Given a charge per area σ on the plates, the electric field *between* the plates is $E = 4\pi\sigma$. Assuming that in field-doped C_{60} the induced charge resides in the top-most layer,⁵ inducing n elementary charges per molecules requires an *external* field (originating from the gate electrode) of $E_{\text{ext}} = 2\pi n/A_{\text{mol}}$, where A_{mol} is the area per molecule in the top-most layer of the crystal. For a C_{60} crystal with lattice constant $a \approx 14$ Å typical areas per molecule are $A_{(111)} = \sqrt{3}a^2/4$ for the (111)-plane and $A_{(001)} = a^2/2$ for the (001)-plane. Even though these areas are quite large, the external fields necessary for field doping are substantial, being of the order of 1 V/Å per induced elementary charge per molecule. This is, however, not the field experienced by a molecule. As C_{60} is highly polarizable ($\alpha \approx 83$ Å³), in the solid, the external field at the site of a molecule is screened by the polarization of the neighboring molecules: A monolayer of dipoles p centered on the lattice sites R_i , generates a field $E_{\text{dip}} = -p \sum_{i \neq 0} |R_i - R_0|^{-3}$ at R_0 , where the

sum is over all sites in the monolayer, except R_0 . For the (111) layer, this sum is about $31.2/a^3$, for the less dense (001) layer it is about $25.6/a^3$. As the dipole moments p of the molecules are induced by the screened field $E_{\text{scr}} = E_{\text{ext}} + E_{\text{dip}}$ at the site of the molecule ($p = \alpha E_{\text{scr}}$), we find, by self-consistent solution, that the external field is reduced by about a factor of two.

Inducing charge and polarizing the molecules is, however, not the only effect of the external field. In addition it also leads to a splitting of the molecular levels — the Stark effect. As the molecular orbitals of C_{60} have a definite parity, a homogeneous field splits the levels only in second order. Thus for low fields the splitting is quite small, but increases quickly for larger fields. We can expect that the splitting of the molecular levels disrupts the electronic structure of the crystal only when it becomes of the order of the band width, which is about $1/2$ eV in C_{60} . Calculations indicate that the splittings of the T_{1u} - and H_u -levels in a *homogeneous* field are surprisingly small, being less than $1/2$ eV up to $E_{\text{scr}} \approx 2$ V/Å (cf. figure 2). Given the crudeness of the argument, it thus seems entirely feasible that doping of a few elementary charges per molecule could be achieved before the electronic structure of the C_{60} is substantially changed.

In the argument above we have described the C_{60} molecules as polarizable points. It is then natural to refine the model by considering also higher multipoles. Such a multipole expansion is particularly suitable for C_{60} as the molecules are nearly spherical. The approach is then the following: First we calculate the response of a C_{60} molecule to external multipole fields. Then we self-consistently solve the electrostatic problem for a lattice of molecules in a homogeneous external field. This provides us with the multipole expansion of the screened field acting on each molecule in the solid. Given that screened field, we can then determine the splitting of the molecular levels as a function of the induced charge.

The organization of the paper reflects this approach: In section II we describe the density functional calculations for determining the multipole response and the Stark splitting for a C_{60} molecule in a multipole field for several symmetrical configuration. Using group theory, in section III, the irreducible parameters for the multipole response are determined. This allows the calculation of the polarization for arbitrary configurations. In section IV we give an analogous treatment for the Stark splittings and explicitly show how the splitting changes as the molecule is rotated relative to the external field. In section V we use these ingredients to self-consistently solve for the screened field seen by a molecule in a charged monolayer. The splitting of the molecular levels in this self-consistent multipole field and the effect of this splitting on the density of states is presented in section VI. Our conclusions are presented in section VII. The methods for calculating the response and splitting for an arbitrarily oriented external field from the results of the density functional calculations that were performed only for special orientations are described in the appendices.

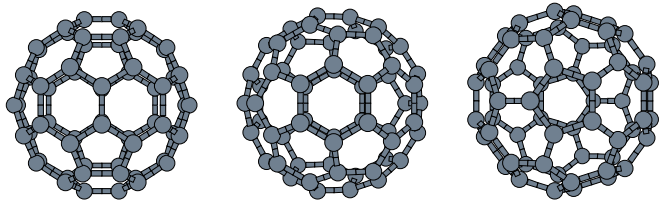


FIG. 1: Orientations of the C_{60} molecule. The coordinate system is chosen such that the x -axis is pointing to the right, the y -axis upward, and the z -axis towards the reader. Thus, from left to right, the molecules are oriented with their 2-, 3-, and 5-fold axis along z . The different orientations are obtained by rotating the molecule about the y -axis: by $\arctan(2 - \tau)$ to go from the first to the second, and by $\arctan(\tau)$ to go from the first to the third orientation. $\tau = (\sqrt{5} + 1)/2$ is the golden ratio.

Appendix A gives an example of how to calculate the response of a molecule using the irreducible parameters derived in section III. In appendix B we derive the coupling matrices needed for the calculating the level splitting when the molecule is rotated in the external field. Finally, appendix C gives the derivation of the matrix describing the field generated by a lattice of identical multipoles at the origin, which is needed for finding the self-consistent electrostatic field.

II. RESPONSE OF A C_{60} MOLECULE

To determine the response of a C_{60} molecule to external multipole fields we have performed all-electron density functional calculations using Gaussian-orbitals.⁶ The basis set comprises 5s4p3d for carbon⁷ and we use the Perdew-Burke-Ernzerhof functional.⁸

In our calculations we apply an external multipole field and study the change in the multipole moments of the charge density and the splitting of the molecular levels as a function of the strength of the external field. To take advantage of the molecule's symmetry we consider multipole fields with the z -axis along the 2-, 3-, and 5-fold axis of the molecule (cf. figure 1). As these axes are each contained in a mirror plane, which we chose to be the x - z -plane, we can treat the thus oriented molecule as having symmetry group C_{2v} , C_{3v} , and C_{5v} respectively. Applying external multipole fields with $l > 0$, this symmetry is maintained if the fields are proportional to the real part of the spherical harmonic Y_{lm} , where m is an integer multiple of the order ($n = 2, 3$, or 5) of the symmetry axis. Likewise, the response of the charge density will only have multipole components proportional to $\text{Re}(Y_{lm})$, with m an integer multiple of n . Calculations were done for such symmetry conserving multipole fields up to $l = 6$. For the 3-fold axis oriented along z , we have, in addition, calculated the response to external fields proportional to $\text{Im}(Y_{5,3})$, $\text{Im}(Y_{6,3})$, and $\text{Im}(Y_{6,6})$, i.e., with a symmetry lowered to C_3 . As we are interested in the linear response,

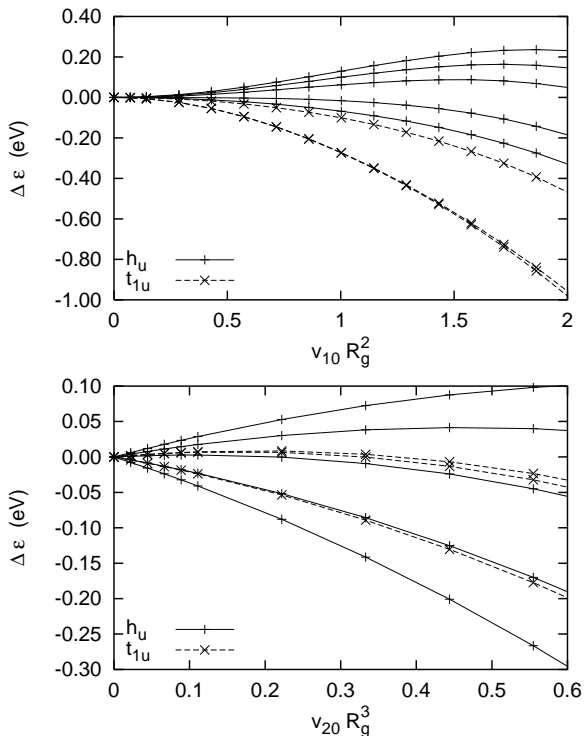


FIG. 2: Splitting of the H_u and T_{1u} levels of a C_{60} -molecule in an external multipole field $V(\mathbf{r}) = V_{lm} R_{lm}^*(\mathbf{r})$ with z along a 2-fold axis. Due to parity, for small external fields, the splitting for $(lm) = (10)$ is quadratic in the external field, while for $(lm) = (20)$ it is linear. The V_{lm} are given in atomic units and $R_g = 7$ bohr. $(lm) = (10)$ corresponds to a homogeneous field with $E_z = -V_{10}$, thus $V_{10} R_g^2 = 1$ in atomic units corresponds to a homogeneous field of about 1 V/\AA .

we have considered small multipole fields and made sure that the calculated response of the charge density is indeed proportional to the strength of the external field. We find that the linear response of a C_{60} molecule is very similar to that of a metallic sphere of radius 4.4 \AA . This effective sphere radius shows a slight increase with l . In addition there are weak off-diagonal terms. To judge the accuracy of our calculation, we have checked how well the selection rules, that are not already imposed by the C_{nv} symmetry, are fulfilled for these off-diagonal terms. From the calculated response, we have determined the irreducible linear response coefficients, which will be given in the next section.

In addition to polarizing the molecule, the external field also splits the degenerate molecular levels of the C_{60} molecule. As the unperturbed molecular orbitals have a definite parity, for a multipole field with odd l there will be no first-order splitting — the quadratic Stark effect. On the other hand, a multipole field with even l can couple states of like parity, so in that case the splitting is linear. This is shown in figure 2. In section IV it will be demonstrated how the splitting of the HOMO- and LUMO-orbitals that were calculated for high-symmetry

geometries can be extended by group theory to arbitrary orientations of the molecule relative to the external multipole field.

All calculations have been performed for the equilibrium geometry of the unperturbed, neutral C_{60} molecule. To estimate the effect of an external field on the shape of the molecule, we have relaxed the structure in the presence of homogeneous external fields of up to 1 V/\AA . We find only small changes (up to about 0.005 \AA) in the lengths of the bonds (1.40 \AA for the short and 1.45 \AA for the long bonds). Likewise, the polarizability changes by less than 1.5%.

Finally, we have calculated the total energy of the isolated C_{60} ion as a function of its charge q (spin unpolarized calculation with relaxed geometries) and extracted the second order term $1/2 U_0 q^2$. To compare with previous calculations,⁹ we find for the polarizability (multipole field with $l = 1$) of the neutral molecule $\alpha = 9.3 \text{ bohr}^3/\text{atom}$, and $U_0 = 3.2 \text{ eV}$.

III. IRREDUCIBLE RESPONSE PARAMETERS

The polarizability α of a molecule describes the linear dependence of the induced dipole moment $\mathbf{p} = \alpha \mathbf{E}$ on the applied electric field \mathbf{E} . For a multipole expansion, α becomes a matrix $\alpha_{l_1 m_1 l_2 m_2}$ describing the response to all multipole fields.¹⁰ To fix the notation (which follows Ref. 10) we briefly review the definition of the multipole response matrix.

The solutions of the Laplace equation $\nabla^2 V(\mathbf{r}) = 0$ are given by

$$V(\mathbf{r}) = V^e + V^i = \sum_{lm} V_{lm} R_{lm}^*(\mathbf{r}) + Q_{lm} I_{lm}^*(\mathbf{r}), \quad (1)$$

where the two terms denote the external potential (V^e), and the induced potential (V^i) due to a charge distribution ρ located around $\mathbf{r} = 0$. Note that both, the Laplace equation as well as the expansion of $V^i(\mathbf{r})$ into multipoles only holds for \mathbf{r} which lie outside the charge distribution. We have introduced the regular and irregular spherical harmonics,¹⁰

$$R_{lm}(\mathbf{r}) = r^l \sqrt{\frac{4\pi}{2l+1}} Y_{lm}(\Omega), \quad (2)$$

$$I_{lm}(\mathbf{r}) = \frac{1}{r^{l+1}} \sqrt{\frac{4\pi}{2l+1}} Y_{lm}(\Omega). \quad (3)$$

Special cases for the regular spherical harmonics are $R_{00} = 1$ and $R_{10} = z$, hence, the external field, $V_{00} = V_0$ corresponds to a constant shift, and $V_{10} = -E_z$ is the z -component of the electric field. For the irregular spherical harmonics we have $I_{00} = 1/r$ and $I_{10} = z/r^3$, thus for the induced potential, $Q_{00} = q$ gives the monopole charge while $Q_{10} = p_z$ is the dipole moment. Generally, the coefficients Q_{lm} are the multipole moments of the

charge distribution ρ

$$Q_{lm} = \int d^3r \rho(\mathbf{r}) R_{lm}(\mathbf{r}). \quad (4)$$

Decomposing the charge distribution $\rho = \rho_0 + \Delta\rho$ into the unperturbed charge density and the change in the charge density due to the external potential, we obtain a decomposition of the multipole moments $Q_{lm} = Q_{lm}^0 + \Delta Q_{lm}$. Within linear response, the coefficients ΔQ_{lm} of the induced multipole moments depend linearly on the coefficients V_{lm} of the external potential, which defines the linear-response matrix $\alpha_{l_1 m_1 l_2 m_2}$:

$$\Delta Q_{l_1 m_1} = - \sum_{l_2 m_2} \alpha_{l_1 m_1 l_2 m_2} V_{l_2 m_2}, \quad (5)$$

where the sign takes into account that the induced fields oppose the external fields. Then $\alpha_{1 m_1 1 m_2}$ gives the dipolar response tensor, while α_{0000} is the self-capacitance U_0 .

The interaction energy of the molecule with the external potential is $E_{\text{ext}} = \int d^3r \rho(\mathbf{r}) V^e(\mathbf{r})$, which, using the previous definitions, reduces to

$$E_{\text{ext}} = \sum_{lm} V_{lm} Q_{lm}^*. \quad (6)$$

Therefore, V_{lm} and Q_{lm} are pairs of conjugate variables and the *total* energy of the molecule as a function of the external field is given by

$$E_{\text{tot}} = -\frac{1}{2} \sum_{\substack{l_1 m_1 \\ l_2 m_2}} \alpha_{l_1 m_1 l_2 m_2} V_{l_1 m_1} V_{l_2 m_2}^* + \sum_{lm} V_{lm} (Q_{lm}^0)^*. \quad (7)$$

Since this is a quadratic form, we see that the matrix α is hermitian. We can make α real and symmetric by unitarily transforming to a real basis (using $\sqrt{2}\text{Re}(Y_{lm})$ and $\sqrt{2}\text{Im}(Y_{lm})$ instead of Y_{lm} and $Y_{l,-m}$ for $m \neq 0$).

The structure of the response matrix α depends on the symmetry of the molecule. For a metallic sphere of radius R the response is isotropic, i.e., α is diagonal in the basis of the spherical harmonics: $\alpha_{l_1 m_1 l_2 m_2} = \delta_{l_1 l_2} \delta_{m_1 m_2} R^{2l_1+1}$. Lowering the symmetry to icosahedral, I_h , introduces some anisotropy. To understand the response matrix for C_{60} we have to consider how the irreducible representations (IR) of the rotation group $SO(3)$ split into IRs of the I_h (see table I). An external multipole field of angular momentum l can only give rise to a response with angular momentum l' , if both IRs of the $SO(3)$ contain a common IR of the I_h . In particular, because of parity, fields with even (odd) l can only give rise to responses with even (odd) l' . Furthermore, as the irreducible representations with $l \leq 2$ are also irreducible with respect to the I_h , for $l \leq 2$ we have $\alpha_{lm lm'} = \alpha_l \delta_{mm'}$. Thus, restricting the multipole expansion to $l \leq 2$, the response of C_{60} is isotropic, with $\alpha_0 \approx 8.1$ bohr, $\alpha_1 \approx 556$ bohr³, and $\alpha_2 \approx 44100$ bohr⁵.

l	I_h
0	A_g
1	T_{1u}
2	H_g
3	$G_u \oplus T_{2u}$
4	$G_g \oplus H_g$
5	$T_{1u} \oplus T_{2u} \oplus H_u$
6	$A_g \oplus T_{1g} \oplus G_g \oplus H_g$

TABLE I: Decomposition of the irreducible representations (IR) of the rotation group $SO(3)$ into the IR of the icosahedral group $I_h \subset SO(3)$.

For $l > 2$ the space spanned by the spherical harmonics Y_{lm} is no longer irreducible with respect to the I_h . Thus we need to find linear combinations of the spherical harmonics that span the irreducible representations of the icosahedral group. We call them Y_{lxk} where l and x denote the IR of the $SO(3)$ and I_h , respectively, while the index k labels the functions within an irreducible representation of the I_h . If in the decomposition an IR x should occur several times, we would have to introduce an additional multiplicity label. However, as can be seen from table I, up to $l = 6$ each IR appears at most once. We therefore suppress the multiplicity label here. Explicit expressions for the basis functions Y_{lxk} , can, e.g., be found in Ref. 12, chapter 16, or Ref. 13, table 4.2.

In the new basis, the matrix α is built of blocks of diagonal matrices

$$\alpha_{l_1 x_1 k_1 l_2 x_2 k_2} = \alpha_{l_1 l_2}(x_1) \delta_{x_1 x_2} \delta_{k_1 k_2}, \quad (8)$$

where $\alpha_{l_1 l_2}(x_1)$ constitute the minimal set of parameters, and, α being real symmetric, $\alpha_{l_1 l_2}(x_1) = \alpha_{l_2 l_1}(x_1)$. The matrix elements of α were calculated up to $l = 6$ using the results of the density functional calculations described in section II. The $\alpha_{l_1 l_2}(x_1)$ are listed in table II. From this minimal set of independent parameters we can determine the response for arbitrary orientations of the C_{60} molecule relative to the external multipole field. An example of how to do this is given in appendix A. The practical advantage of this procedure is clear: We only need to perform density functional calculations for a number of highly symmetric configurations, for which the numerical effort is much reduced. Using group theory the response for arbitrary configurations can then be determined from these special cases.

Note that the group theoretical approach presented in this section is particularly elegant in the case of a neutral molecule which has icosahedral symmetry. Upon charging, orbitals become partially filled and the symmetry is reduced which leads to a higher number of irreducible response coefficients. Furthermore, the symmetry of a charged molecule depends on how the additional charge arranges in the degenerate orbitals. This is a subtle question in the case of an isolated C_{60} molecule and involves Jahn-Teller effects and Coulomb interaction in competition¹¹. In the present work we restrict the analysis to neutral molecules.

	$\frac{\alpha_{l_1 l_2}(x)}{R_0^{l_1+l_2+1}}$	$\frac{\alpha_{l_1 l_2}(x)}{R_0^{l_1+l_2+1}}$
$\alpha_{00}(A_g)$	1.019	$\alpha_{55}(T_{1u})$ 1.707(9)
$\alpha_{11}(T_{1u})$	0.990(0)	$\alpha_{55}(T_{2u})$ 1.430(4)
$\alpha_{22}(H_g)$	1.154(0)	$\alpha_{55}(H_u)$ 2.031(13)
$\alpha_{33}(G_u)$	1.268(1)	$\alpha_{15}(T_{1u})$ -0.077(5)
$\alpha_{33}(T_{2u})$	1.376(3)	$\alpha_{35}(T_{2u})$ 0.039(6)
$\alpha_{44}(H_g)$	1.542(6)	$\alpha_{66}(A_g)$ 1.598(5)
$\alpha_{44}(G_g)$	1.477(9)	$\alpha_{66}(H_g)$ 1.209(21)
$\alpha_{24}(H_g)$	0.074(6)	$\alpha_{66}(G_g)$ 1.964(2)
		$\alpha_{66}(T_{1g})$ 2.503
		$\alpha_{26}(H_g)$ -0.023(13)
		$\alpha_{46}(H_g)$ 0.195(12)
		$\alpha_{46}(G_g)$ -0.337(13)

TABLE II: Linear response coefficients of a neutral C_{60} molecule derived from the results of our density functional calculations. The matrix elements $\alpha_{l_1 l_2}(x)$ are normalized with $R_0 = 8.25$ bohr. By comparing matrix elements determined from the response to potentials applied along the 2-, 3-, and 5-fold axis, we have determined, wherever possible, the uncertainties in the values of the matrix elements. The value of $\alpha_{00}(A_g)$ is given by the quadratic term of the change of the ground state energy upon charging of the molecule.

	T_{2u} ———	-2.24 eV	
	T_{1g} ———	-3.10 eV	
LUMO	T_{1u} ———	-4.20 eV	
----- E_F			
HOMO	H_u ———	-5.83 eV	
	G_g ———	-6.99 eV	
	H_g ———	-7.12 eV	
	G_u ———	-8.66 eV	

FIG. 3: Energy levels of the C_{60} molecule as calculated by density functional theory. The Fermi energy for the undoped molecule is indicated.

IV. LEVEL SPLITTING

In this section, a minimal set of parameters describing the Stark effect in a neutral molecule is deduced using the Wigner-Eckart theorem for the icosahedral symmetry¹². This is achieved in the framework of density-functional perturbation theory¹⁶ where an external perturbation V induces a change in the effective potential (self-consistent field) V^{eff} which couples the degenerate energy levels. In linear order the change is given by

$$\Delta V^{\text{eff}}(\mathbf{r}) = V(\mathbf{r}) + \Delta V^i(\mathbf{r}) + \left. \frac{dv_{\text{xc}}}{dn} \right|_{n=n(\mathbf{r})} \Delta n(\mathbf{r}), \quad (9)$$

where $\Delta V^i(\mathbf{r}) = e^2 \int d\mathbf{r}' \Delta n(\mathbf{r}') |\mathbf{r} - \mathbf{r}'|^{-1}$ is the change in the induced potential due to the linear change $\Delta n(\mathbf{r})$ in the electron distribution. The last term is the exchange-correlation potential. Within linear response, the change in the charge distribution Δn as well as the induced potential ΔV^i have the same symmetry (with respect to I_h) as the external perturbation V^e . Furthermore, if

$n(\mathbf{r})$ is the unperturbed charge distribution, then the factor $\left. \frac{dv_{\text{xc}}}{dn} \right|_{n=n(\mathbf{r})}$ in the last term of (9) has A_g symmetry and does not change the symmetry of Δn . Consequently, ΔV^{eff} has the same symmetry as V^e and, using the notation of the previous section, can be written as

$$\Delta V^{\text{eff}}(\mathbf{r}) = \sum_{l x k} V_{l x k} f_{x k}^l(\mathbf{r}) + \mathcal{O}[V_{l x k}^2], \quad (10)$$

where $f_{x k}^l(\mathbf{r})$ are partner functions of the IR x of I_h . Note that $f_{x k}^l$ contains spherical harmonics $Y_{l' x k}$ with all l' allowed by table I. The coupling of the degenerate levels is given by the matrix elements of ΔV^{eff} with respect to the eigenstates of the unperturbed molecule which are denoted by $|n x k\rangle$, where n is the quantum number differentiating between orbitals with the same IR x . In this context, the functions $f_{x k}^l$ play the role of tensor operators of I_h and the Wigner-Eckart theorem can be used to write the matrix elements as

$$\langle n_2 x_2 k_2 | \Delta V^{\text{eff}} | n_1 x_1 k_1 \rangle = \sum_{l x k} V_{l x k} \sum_{\lambda} t_{\lambda}(n_1 x_1 n_2 x_2; l x) C_{k_2 k_1}^k(\lambda; x_2 x_1; x). \quad (11)$$

The coefficients $C_{k_2 k_1}^k(\lambda; x_2 x_1; x)$ denote the 3jm symbols (or Clebsch-Gordan coefficients) of I_h and are entirely determined by the icosahedral symmetry. In the present work they were taken from Ref. 12 and are discussed in detail in appendix B. In order for $C_{k_2 k_1}^k(\lambda; x_2 x_1; x)$ to be non-zero, the IR x needs to be present in the decomposition of $x_1 \otimes x_2$. If x occurs more than once in $x_1 \otimes x_2$ then the multiplicity index λ is required. From this selection rule follows again that even potentials couple linearly whereas odd potentials couple only in second order (quadratic Stark effect). Finally, the factors $t_{\lambda}(n_1 x_1 n_2 x_2; l x)$ are the coupling constants which constitute the minimal set of parameters describing the level splitting.

We analyze in more detail the level splitting of the LUMO ($x = T_{1u}$) and HOMO ($x = H_u$) for $l = 1$ and $l = 2$ external potentials which correspond to an electric field and a quadrupole potential. We will see in Section V that these two multipoles are dominant in the case of a charged C_{60} layer exposed to an electric field. Within the icosahedral symmetry I_h , the two potentials form partners for the IR T_{1u} and H_g respectively (see table I). Details of the calculation are given in appendix B. The coupling constant derived from the level splitting calculated by DFT are given in table III. In the case of the odd $l = 1$ potential, only second-order coupling to closest-by orbitals was considered (T_{1g} for the LUMO, H_g and G_g for the HOMO, see figure 3), which, however, as shown below, gives very satisfactory results. For the splitting of the HOMO under the $l = 2$ ($x = H_g$) potential, there are two coupling constants because H_g occurs twice in the product $H_u \otimes H_u = A_g \oplus T_{1g} \oplus T_{2g} \oplus 2G_g \oplus 2H_g$. In appendix B the coupling matrix $H'_{T_{1u}}$ (H'_{H_u}) describing the level splitting of the LUMO (HOMO), due to an applied $(lm) = (10)$ and $(lm) = (20)$ potential along an

x_1	x_2	x	λ	$t_\lambda(x_1 x_2; x)$
T_{1u}	T_{1g}	T_{1u}		-0.663
	T_{1u}	H_g		-0.225
H_u	H_g	T_{1u}		-0.730
	G_g	T_{1u}		-0.730
	H_u	H_g	1	-0.520
	H_u	H_g	2	-0.018

TABLE III: Coupling constants $t_\lambda(x_1 x_2; l)$ as defined by equation (11) (indices n_1, n_2, l are dropped) among the energy levels near the Fermi energy. The coupling constants are given in units of eV $(7 \text{ bohr})^{l+1} e^{-1}$ where $l = 1$ for $x = T_{1u}$ and $l = 2$ for $x = H_g$. The negative sign of the coefficients is due to the negative charge of the electrons. Note that the coupling constants $t(H_u H_g; T_{1u})$ and $t(H_u G_g; T_{1u})$ are equal up to the third digit which is due to fact that the H_g and G_g levels have almost the same radial dependence because of the their closeness in energy (see Fig 3).

arbitrary direction of the molecule, is calculated using perturbation theory. To a very good approximation, the result can be cast into the form

$$H'_{T_{1u}}(\theta) = \left(V_{10}^2 c_1 + V_{20} c_2 \right) \mathcal{C}_{T_{1u}}(\theta), \quad (12)$$

$$H'_{H_u}(\theta) = \left(V_{10}^2 d_1 + V_{20} d_2 \right) \mathcal{C}_{H_u}(\theta), \quad (13)$$

where c_1, c_2, d_1 and d_2 are constants depending on the coupling constants of table III and the energies given in figure 3. $\mathcal{C}_{T_{1u}}(\theta)$ and $\mathcal{C}_{H_u}(\theta)$ are matrices within the LUMO and HOMO subspace respectively and depend on the angle θ between the z -direction of the $(lm) = (10), (20)$ potentials and the 5-fold axis of the molecule. (for more details see appendix B). In figure 4 and figure 5 the splitting of the LUMO and HOMO is shown using the previous relations along with the points calculated by DFT. The group-theoretical fit is very satisfactory. Note that the splitting of the LUMO is independent of the orientation of the molecule when only coupling among the LUMO or to the T_{1g} is considered (see appendix B). Furthermore, relations (12) and (13) are quite remarkable, as they imply that the contributions of the $l = 1$ and $l = 2$ potential lift the degeneracy of the molecular levels in the same way, and thus the total splitting is given by the sum of the $l = 1$ and $l = 2$ splittings.

V. MOLECULES IN A LAYER

In this section a simple model of a C_{60} FET is considered. As mentioned above a FET can be understood as capacitance where one plate is the gate and the other plate is the material (here C_{60}) which is investigated. An analysis of this device, in particular the calculation of the charge distribution, was done in a previous work⁵. It was found, that the charge concentrates on the first layer in the high doping regime. In what follows, we take this as a motivation to consider a single layer of C_{60} molecules

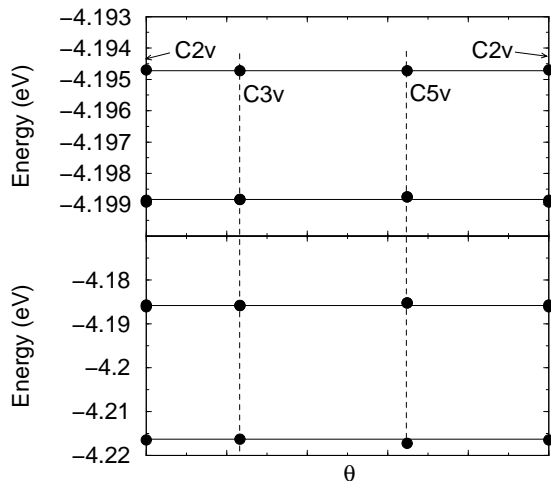


FIG. 4: Splitting of the LUMO for an $(lm) = (10)$ and $(lm) = (20)$ potential as the molecule is rotated by $\pi/2$ about the y -axis. The orientations shown in figure 1 are indicated. The splitting calculated with DFT at these high symmetry orientations are indicated by the filled symbols. The lines give the result of perturbation theory, fitted to the calculation for the 3-fold axis. *Upper panel:* $(lm) = (10)$ potential with $V_{10} = 0.143 e (7 \text{ bohr})^{-2}$. The lower level is twofold degenerate. *Lower panel:* $(lm) = (20)$ potential with $V_{20} = 0.180 e (7 \text{ bohr})^{-3}$. The upper level is twofold degenerate.

which acts as a plate of a capacitance. We use the response of a *neutral* molecule (table II) to describe the electrostatic behavior of the molecules in the layer. The doped charge is taken care of by adding a monopole on every site. The molecules are then exposed to the electric field arising from the gate as well as the monopole fields of the neighboring molecules. In order to simplify the calculation, we assume a perfect lattice, either square, for the (001), or triangular, for the (111) plane of the fcc lattice formed by the C_{60} molecules in the bulk. In order for the sites to be equivalent we neglect the non-spherically symmetric part of the response of the C_{60} -molecule and use the averaged response given by

$$\alpha_{l_1 m_1 l_2 m_2}^{\text{spher.-sym.}} = \delta_{l_1 l_2} \delta_{m_1 m_2} \sum_{xk} \frac{\alpha_{l_1 x k l_1 x k}}{2l_1 + 1}, \quad (14)$$

where the sum is taken over all components of the l_1 subspace. Since the response of C_{60} for multipoles $l \leq 2$ is isotropic (cf. section III), this averaging is exact for $l = 1, 2$.

Because of translational invariance, the total potential is given by

$$V_{\text{tot}}(\mathbf{r}) = V^e(\mathbf{r}) + \sum_{\mathbf{R}_i} V^i(\mathbf{r} - \mathbf{R}_i), \quad (15)$$

where the sum is taken over all lattice sites \mathbf{R}_i . At a given site, say $\mathbf{R}_i = 0$, the total potential can also be decomposed as $V_{\text{tot}}(\mathbf{r}) = V^{\text{scr}}(\mathbf{r}) + V^i(\mathbf{r})$ where the screened

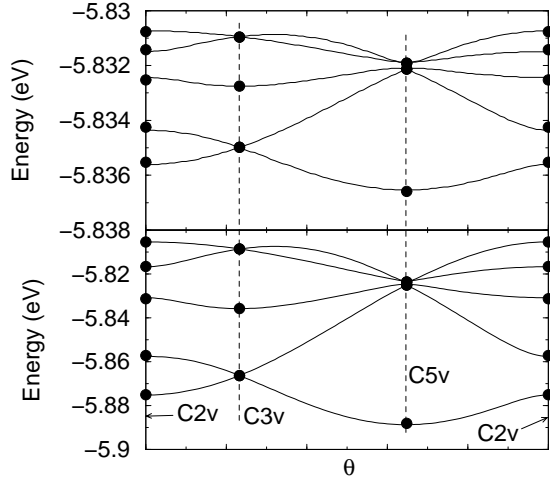


FIG. 5: Splitting of the HOMO for an $(lm)=(10)$ and $(lm)=(20)$ potential. See figure 4 for more details. In this plot the similarity of the splitting resulting from the different potentials (cf. eqn. (13)) is particularly striking.

potential $V^{\text{scr}}(\mathbf{r}) = V^e(\mathbf{r}) + \sum_{\mathbf{R}_i \neq 0} V^i(\mathbf{r} - \mathbf{R}_i)$ contains the external potential $V^e(\mathbf{r})$ as well as the sum of all induced potentials of the other molecules. This sum depends linearly on the induced potential V^i and, hence, the coefficients of V^{scr} are given by

$$V_{l_1 m_1}^{\text{scr}} = V_{l_1 m_1} + \sum_{l_2 m_2} \beta_{l_1 m_1 l_2 m_2} Q_{l_2 m_2}. \quad (16)$$

The matrix β is entirely given by geometry and discussed in appendix C. On the other hand, the screened potential V^{scr} induces a potential ΔV^i as given in equation (5). Therefore the total induced potential $V^i = V^{i,0} + \Delta V^i$ is

$$Q_{l_1 m_1} = Q_{l_1 m_1}^0 - \sum_{l_2 m_2} \alpha_{l_1 m_1 l_2 m_2} V_{l_2 m_2}^{\text{scr}}. \quad (17)$$

Equations (16) and (17) can be combined by eliminating the coefficients Q_{lm} which yields

$$V_{l_1 m_1}^{\text{scr}} = \sum_{l_2 m_2} [1 + \beta \alpha]_{l_1 m_1 l_2 m_2}^{-1} V_{l_2 m_2}^{\text{bare}}, \quad (18)$$

$$V_{l_1 m_1}^{\text{bare}} = V_{l_1 m_1} + \sum_{l_2 m_2} \beta_{l_1 m_1 l_2 m_2} Q_{l_2 m_2}^0, \quad (19)$$

where the $V_{l_1 m_1}^{\text{bare}}$ describes the bare potential arising from the external potential (the electric field of the gate) and intrinsic moments of the molecules (the induced charge, i.e. monopoles). The square (triangular) lattice in the presence of the electric field has the rotational symmetry C_{4v} (C_{6v}). As a consequence, only components with these symmetries are non-zero and therefore they are given by $\text{Re}(Y_{lm})$ with m a multiple of 4

lm	square		triangular	
	v_{lm}^{bare}	v_{lm}^{scr}	v_{lm}^{bare}	v_{lm}^{scr}
10	0.862	0.499	0.996	0.530
20	-0.230	-0.189	-0.280	-0.219
30	0	0.039	0	0.053
40	0.0133	0.0030	0.0177	0.0015
4c4	0.0174	0.0097	-	-

TABLE IV: Components of the bare and screened potential for the square and triangular lattice with $a/\sqrt{2} = 10 \text{ \AA}$. The coefficients are in units of $q/(7 \text{ bohr})^{l+1}$, where q is the charge per C_{60} molecule. Note that $7 \text{ bohr} \approx 3.7 \text{ \AA}$ is about the radius of the C_{60} molecule.

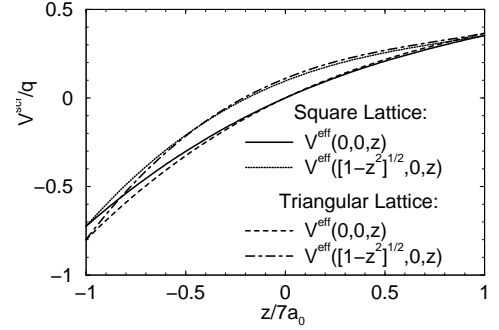


FIG. 6: Screened potential V^{scr} across the layer with the parameters from Tab IV for the square and triangular lattice. The gate is assumed to be on the left. The lower lines correspond to a cut through the center of the molecule whereas the upper lines are along half-circles with the radius of the molecule ($7 \text{ bohr} \approx 3.7 \text{ \AA}$).

(6). Using relation (18) and (19) the screened potential can be calculated. The non-zero components entering (19) are the monopole charge $Q_{00}^0 = q$ and electric field $V_{10} = -E_{\text{Gate}}$. As the FET is overall neutral $E_{\text{Gate}} = -2\pi q/A_{\text{mol}}$ with $A_{(001)} = a^2/2$ for the square lattice and $A_{(111)} = \sqrt{3}a^2/4$ for the triangular lattice. The results are given in table IV and graphically depicted in figure 6. The components $(lm) = (10), (20)$ are most dominant and higher ones are at least one order of magnitude smaller. This justifies a posteriori the assumption of spherical symmetry because (14) is exact for $(lm) = (10), (20)$. From figure 6 it can be seen that the electric field is efficiently screened within the layer. Note that decrease of the electric field yields negative sign of v_{20} in table IV. We also have checked the influence of adjacent layers of C_{60} and of a close-by dielectric (with a dielectric constant $\epsilon = 10$). The effects on the parameters in table IV were less than 2%. The reason is that the field inhomogeneities induced by a 2D lattice of multipoles decay exponentially outside the lattice.

VI. SPLITTING IN SELF-CONSISTENT MULTIPOLE FIELD

We are now in the position to estimate the effect of the external field on the electronic structure of the C_{60} molecules in the monolayer that carries charge. To do so we have performed density functional calculations for a molecule in the self-consistent multipole fields as determined in the previous section (cf. table IV). Figure 7 shows the splitting of the molecular levels in the self-consistent field for a (001) monolayer, where the molecule is oriented with one of its two-fold axes pointing in the direction of the external field. The maximum energy difference between split states is given in table V and compared to the result from the perturbative formula (12) and (13), which is in good agreement for $|q| \leq 2$. As figure 8 demonstrates, similar results are obtained for other geometries. Qualitatively, the results are also in agreement with an approximative tight-binding calculation published earlier in Ref. 17. As expected we find that the stronger the external field, i.e., the larger the induced charge, the stronger the splitting. We notice also a pronounced asymmetry in the splitting: when the monolayer is charged with electrons the splitting is different from when it is charged with holes. Again, the reason is parity: Because of parity an external homogeneous field, and more generally any multipole potential with l odd, leads to a quadratic Stark effect. Hence, for odd l the splitting is independent of the sign of the field. For l even, however, the levels split already in first order (linear Stark effect), so the splitting changes sign with the external field. Thus the asymmetry originates from the multipoles with even l . Moreover, because of the first-order versus second-order effect, even though the largest even multipole (20) is significantly smaller than the largest odd multipole (the screened external field), it contributes considerably to the splitting.

We have seen in section IV that for the HOMO and LUMO of C_{60} the splittings caused by (10) and (20) multipole potentials are essentially additive (cf. equation (11)). Thus we expect them to add up for one sign of the external field, while they should compensate for the opposite sign. In fact, for electron doping the splittings of the HOMO seem to almost perfectly cancel, while upon hole doping the splitting of the HOMO is essentially doubled compared to the splitting caused by the screened homogeneous field alone. Thus for the HOMO, the splittings happen to add up for an external field that induces charge carriers into that orbital — a situation that is particularly unfavorable for hole doping. For the LUMO the situation is similar: For an external field that induces electrons in the LUMO the splitting is enhanced. So it turns out that the contributions of the higher multipoles conspire to enhance the splitting of the orbital that carries the induced charge. For both, HOMO and LUMO, the splitting becomes comparable to the respective band width for a field that corresponds to about two charge carriers per molecule.

q	LUMO		HOMO	
	DFT	Pert.	DFT	Pert.
-2e	0.312	0.305	0.049	0.001
-1e	0.105	0.102	0.062	0.060
0	0	0	0	0
1e	0.006	0.002	0.178	0.179
2e	0.057	0.097	0.455	0.476
3e	0.151	0.297	0.779	0.892

TABLE V: Maximum energy difference (in eV) between split HOMO and LUMO states, respectively, as a function of doping q of the square lattice. 2nd and 4th column are the DFT results from figure 7. 3rd and 5th column are calculated by perturbation theory as described in section IV.

The calculations reported above have been performed for an uncharged molecule. Considering instead the splitting for a molecule that carries the proper induced charge, the splittings are substantially reduced. This is easily understood: Due to the splitting, the electrons will fill only the lowest of the split levels. But since the interaction between electrons in the same orbital is larger than the interaction of electrons in different orbitals, the occupied levels will be shifted upwards, compared to the levels that were left empty — thereby reducing the splitting. We are, however, not interested in the splitting per se, but in the effect of the splitting on the band structure of a monolayer. Thus allowing electrons only in the energetically lowest levels would mean that in the lattice, the electrons are not allowed to hop to energetically higher ones of the split levels. This implies that the original band structure would already be separated into a set of bands originating from occupied, and another set of bands originating from the empty orbitals. To eliminate the undesired differences in the interaction between electrons in the split orbitals, we therefore work with the splittings obtained for a neutral molecule.

To estimate the effect of the Stark splitting on the density of states (DOS), we have performed tight-binding calculations for the (001) monolayer (square lattice), assuming the unidirectional structure (two-fold axis of the molecules pointing in the direction of the external field). The basis for the tight-binding Hamiltonian and the hopping matrix elements were taken from the parametrization given in Ref. 18. The splittings shown in figure 7 were then used to derive an on-site coupling between the different orbitals. In the case of the LUMO, the on-site coupling is diagonal and reduces to orbital dependent on-site energies. The DOS for the LUMO (T_{1u}) and the HOMO (H_u) bands calculated with this model for different charging are shown in figure 9 and 10, respectively. We find that already for an induced charge of one carrier per molecule the change with respect to the unperturbed DOS is sizable. For $q = -2$ one of the T_{1u} -bands is already completely separated from the other two. Also the HOMO density of states shows for $q = 2$ hardly any resemblance to the original DOS, and for $q = 3$ also the H_u -bands fall into two groups. We thus conclude that

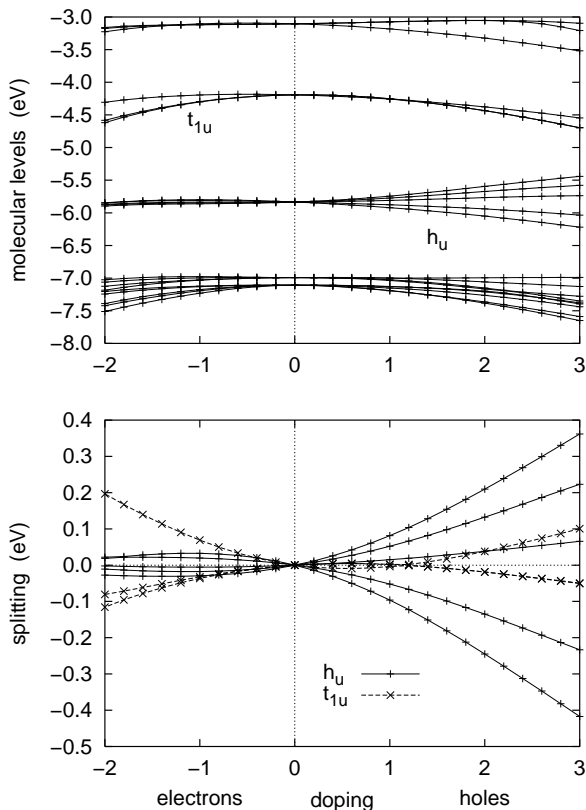


FIG. 7: Splitting of the molecular levels of a C_{60} molecule in the self-consistent multipole potential ($l \leq 2$) for a (001) monolayer (square lattice) in a homogeneous external field as a function of the induced charge. The molecule is oriented such that one of its two-fold axis points in the direction of the external field (perpendicular to the monolayer). The top panel shows the positions of the split (from bottom to top) H_g , G_g , H_u , T_{1u} , and T_{1g} levels. The bottom gives the splitting of the H_u (HOMO) and T_{1u} (LUMO) levels relative to their respective center of gravity.

beyond filling $|q| = 2$ the electronic structure is distorted so much compared to the unperturbed monolayer that one can no longer speak of doping.

The calculation of the density of states in a minimal tight-binding basis involves, of course, approximations: First, in the lattice, not only hopping between LUMO (HOMO) levels is allowed, but also hopping via energetically close-by levels. An orbital at $\Delta\varepsilon$ away will give a contribution to the hopping of about $t^2/\Delta\varepsilon$, where t is the hopping matrix element from the orbital, that we consider explicitly, to the orbital at $\Delta\varepsilon$. The influence of this effect on the hopping between molecules was studied in Ref. 18 and changes of the order of 5% were found. More importantly, due to the deformation of the molecular orbitals in the field, the hopping matrix elements between the HOMO or LUMO orbitals will change. For a simple estimate, we have performed tight-binding calculations of a C_{60} molecule in an external homogeneous field and determined the average hopping matrix element between the t_{1u} -orbitals following the approach of Ref. 19. We

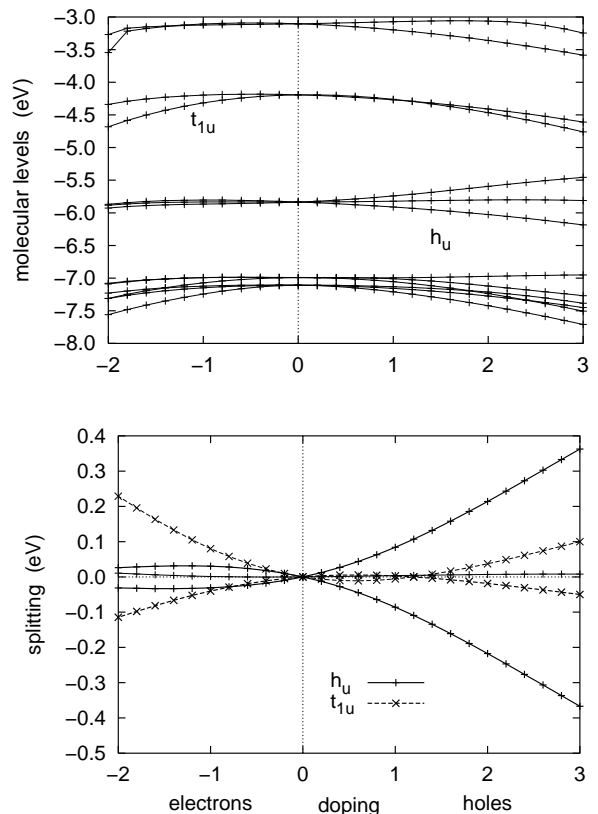


FIG. 8: Splitting of the molecular levels of a C_{60} molecule in the self-consistent multipole potential ($l \leq 2$) for a (111) monolayer (triangular lattice) in a homogeneous external field as a function of the induced charge. The molecule is oriented such that one of its three-fold axis points in the direction of the external field (perpendicular to the monolayer). Otherwise the plots are as in figure 7. The thick lines in the lower panel indicate the two-fold degenerate levels.

find that the change in the hopping matrix elements depends strongly on the orientation of the molecules. Typical changes are of the order of 10–20%.

VII. CONCLUSIONS

We have analyzed the changes in the electronic structure of a C_{60} monolayer in which charge carriers are induced by the application of an external homogeneous electric field. We find that the effective field seen by each molecule in the monolayer is strongly screened, but that there are additional higher multipole potentials. Although these components are considerably weaker than the screened homogeneous field, for even l , they give a significant contribution to the level splitting as they are of first order. In addition the $l = 1$ (homogeneous field) and $l = 2$ potentials split the HOMO and LUMO in almost the same way, so the splittings they produce add up or counteract, depending on the sign of the external field. For both, the HOMO and the LUMO, the signs turn out to be such, that the splitting is enhanced when the charge

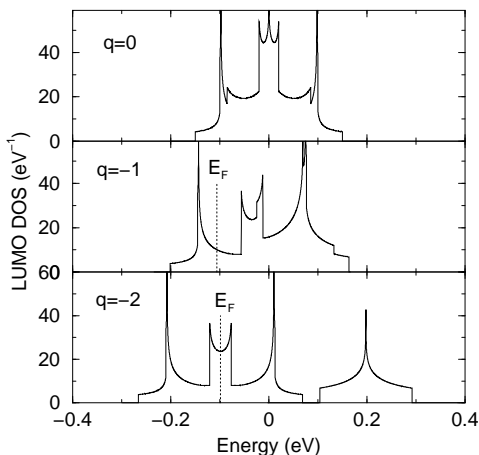


FIG. 9: DOS (per molecule and for both spins) of the LUMO-band taking into account the level splitting for doping $q = 0, -1, -2$. The Fermi energy is indicated.

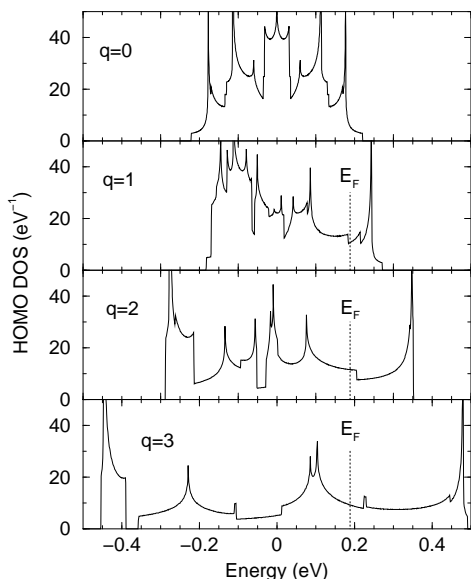


FIG. 10: As in figure 9 but for the DOS of the HOMO-band with $q = 0, 1, 2, 3$.

is induced in the respective level. Thus the level that carries the field-induced charge is strongly changed by the effective field — a particularly unfavorable situation if one wants to achieve doping, i.e., filling of a level without substantially changing its electronic structure.

There are, of course, some effects that have been neglected in our analysis: The polarizability of C_{60} increases when charge is put in the T_{1u} orbital. Thus when filling the LUMO the screening of the external field should become somewhat more efficient. Second, due to the electric field the molecular orbitals are deformed and thus the hopping matrix elements between neighboring molecules change. This effect depends sensitively on

the orientation of the molecules but it typically leads to a slight decrease of the band width with applied field, making the Stark splitting even more important. Furthermore we have neglected the effect of electron-phonon coupling, which also tends to narrow the bands. This should be particularly important for the H_u -band.²⁰ Finally, we have not considered correlation effects. It is known that, at integer filling, the alkali-doped Fullerenes are close to a Mott transition and that they are metallic because of orbital degeneracy.²² Due to the reduced coordination in two dimensions, a doped monolayer of C_{60} should be even more strongly correlated, even if the orbitals are still degenerate. Lifting the degeneracy, e.g., by the Stark effect significantly increases correlations even further.²¹ It therefore seems inevitable that for an integer number of induced charges a C_{60} monolayer will be a Mott insulator, even though it is not clear what effect the gate oxide might have on the Coulomb repulsion U between two electrons on a C_{60} molecule.²³

To summarize, it seems safe to conclude that the physics of field-effect devices based on C_{60} as active material should be quite different from that of the alkali-doped fullerenes, at least at doping levels beyond two carriers per molecule.

Acknowledgments

The authors would like to thank O. Gunnarsson, T.M. Rice, B. Batlogg, and C. Helm for fruitful discussions. This work has been supported by the Swiss Nationalfonds.

APPENDIX A: RESPONSE FOR GENERAL ORIENTATION

To illustrate the use of the response coefficients given in table II, we show, how to calculate the response for a multipole potential with $(lm) = (30)$ for different orientations of the z -axis with respect to the C_{60} molecule. This is the first non-trivial case, as the response for multipoles with $l \leq 2$ is isotropic. To start with, we need the basis functions $Y_{l_x k}$ spanning the irreducible representation of the I_h , that were introduced in section III. For specific orientations, these can be found, e.g., in the Ref. 12, chapter 16, or Ref. 13, table 4.2. For arbitrary orientations, they have to be derived by explicitly finding the basis functions that span the irreducible representations of the icosahedral group. For the sake of the example, we consider the response for z along the 5-fold and the 3-fold axis of the C_{60} molecule. The corresponding basis functions are then both found in Ref. 12. Since we are interested in the response to an external multipole with $(lm) = (30)$, we have to identify those basis functions that contain Y_{30} . They are shown in table VI. It turns out that for z parallel to the 5-fold axis the $(lm) = (30)$ potential corresponds to a pure T_{2u} potential. Thus the

IR of I_h	5-fold axis	3-fold axis
G_u	-	$\frac{2\sqrt{2}}{3}Y_{30} - \frac{1}{3}Y_{3c3}$
T_{2u}	$-Y_{30}$	$-\frac{1}{3}Y_{30} - \frac{2\sqrt{2}}{3}Y_{3c3}$

TABLE VI: Transformed $l = 3$ spherical harmonics, which are partner functions for the IR of I_h and which contain Y_{30} . The second (third) column is for the case where the 3-fold (5-fold) axis of the molecule is parallel to the z -axis. The real spherical harmonic is $Y_{3c3} = \sqrt{2} \text{Re}(Y_{33})$.

response is given by $\Delta Q_{30} = \alpha_{33}(T_{2u}) V_{30}$. For z along

the 3-fold axis the situation is more complicated, as the potential is now a mixture of partner functions of G_u and T_{2u} : As can be seen from table VI, it mixes with the $Y_{3c3} = \sqrt{2} \text{Re}(Y_{33})$ component. By construction, the response matrix α in the subspace spanned by $\{Y_{30}, Y_{3c3}\}$ is diagonal, with diagonal elements $\alpha_{33}(H_u)$ and $\alpha_{33}(T_{2u})$, when written in the basis functions listed in table VI. However, to obtain the multipole response we have to use the basis (Y_{30}, Y_{3c3}) , for which there are off-diagonal elements:

$$\alpha = \frac{1}{9} \begin{pmatrix} 8\alpha_{33}(H_u) + \alpha_{33}(T_{2u}) & \sqrt{8}[\alpha_{33}(T_{2u}) - \alpha_{33}(H_u)] \\ \sqrt{8}[\alpha_{33}(T_{2u}) - \alpha_{33}(H_u)] & \alpha_{33}(H_u) + 8\alpha_{33}(T_{2u}) \end{pmatrix}. \quad (\text{A1})$$

We thus find

$$\begin{aligned} \Delta Q_{30} &= \frac{1}{9} [8\alpha_{33}(H_u) + \alpha_{33}(T_{2u})] V_{30}, \\ \Delta Q_{3c3} &= \frac{\sqrt{8}}{9} [\alpha_{33}(T_{2u}) - \alpha_{33}(H_u)] V_{30}. \end{aligned}$$

APPENDIX B: COUPLING MATRICES

In this section we discuss the calculation of the level splitting for arbitrary directions within perturbation theory using the coupling constants of table III. As discussed above, we restrict the analysis to $l = 1$ and $l = 2$ external potentials, which corresponds to $x = T_{1u}$ and $x = H_g$ potentials in the icosahedral symmetry I_h . In first order perturbation theory, the splitting of the levels in the degenerate subspace \mathcal{E}_{nx} is given by the eigenvalues of the matrix

$$H_{k_1 k_2}^{(1)}(nx) = \langle nx k_2 | V^{\text{eff}} | nx k_1 \rangle. \quad (\text{B1})$$

This matrix vanishes in the case of an odd potential and the splitting is given by the second order expression

$$H_{k_1 k_2}^{(2)}(nx) = \sum_{\substack{(n' x') \\ \neq (nx)}} \sum_{k'} \frac{\langle nx k_2 | V^{\text{eff}} | n' x' k' \rangle \langle n' x' k' | V^{\text{eff}} | nx k_1 \rangle}{E_{nx} - E_{n' x'}}. \quad (\text{B2})$$

The matrix-elements in (B1) and (B2) are given in (11) and involve the icosahedral Clebsch-Gordan coefficients $\mathcal{C}_{k_2 k_1}^k(\lambda; x_2 x_1; x)$. In order for the k -indices to be defined we consider the molecule oriented with the 5-fold axis parallel to the z -axis (see figure 1). This allows to label the states within a multiplet unambiguously with its C_5 index k . The ordered basis of a T_{1u} subspace has k -indices $(0, 1, -1)$ whereas the ordered basis of an H_u subspace is given by $(0, 1, -1, 2, -2)$. Note that in the case of applied $l = 1$ or $l = 2$ potential, the k index corresponds to the m index of the spherical harmonics. For a detailed discussion we refer to Ref. 12. We will present the coefficients $\mathcal{C}_{k_2 k_1}^k(\lambda; x_2 x_1; x)$ as matrices with respect to the indices k_1 and k_2 . In order to reduce the number of matrices, we will give the coupling matrices for $(lm) = (10), (20)$ potentials, which are rotated around the y -axis by an angle θ . The resulting matrices are then given by

$$\mathcal{C}^\theta(\lambda; x_2 x_1; x) = \sum_k R_{0k}^l(\theta) \mathcal{C}^k(\lambda; x_2 x_1; x), \quad (\text{B3})$$

where $R_{k'k}^l(\theta)$ is the rotation matrix of the spherical harmonics in a given l -subspace. Using the previous relations and equation (11), the coupling matrix for an even $l = 2$ potential is given by

$$H^{(1)}(nx, \theta) = V_{20} \sum_\lambda t_\lambda(nx, nx; H_g) \mathcal{C}_\lambda^\theta(x; H_g). \quad (\text{B4})$$

Note that the multiplicity label λ is only relevant for the HOMO H_u because H_g occurs twice in the product $H_u \otimes H_u = A_g \oplus T_{1g} \oplus T_{2g} \oplus 2G_g \oplus 2H_g$. The coupling matrix for the odd $l = 1$ potential is

$$H^{(2)}(nx, \theta) = V_{10}^2 \sum_{\substack{(n'x') \\ \neq (nx)}} \frac{t(nx \ nx'; T_{1u})^2}{E_{nx} - E_{n'x'}} \mathcal{C}^\theta(xx'; T_{1u})^\top \mathcal{C}^\theta(xx'; T_{1u}). \quad (\text{B5})$$

In the following we restrict the sum over subspaces $\mathcal{E}_{n'x'}$ closest in energy to \mathcal{E}_{nx} which is the T_{1g} subspace in the case of the LUMO and the H_g and G_g subspaces in the case of the the HOMO (see Fig 3). Below, the coupling matrices $\mathcal{C}_\lambda^\theta(x_1 x_2; x)$ which are needed to calculate the splitting of the HOMO and LUMO are given. They are traceless $\text{Tr} \mathcal{C}^\theta = 0$ and normalized such that $\text{Tr} (\mathcal{C}^\theta)^\top \mathcal{C}^\theta = 1$. The coupling matrices which describe the splitting of the LUMO are

$$\mathcal{C}^\theta(T_{1u} T_{1g}; T_{1u}) = \frac{1}{2} \begin{pmatrix} 0 & -\sin \theta & -\sin \theta \\ -\sin \theta & -\sqrt{2} \cos \theta & 0 \\ -\sin \theta & 0 & \sqrt{2} \cos \theta \end{pmatrix}, \quad (\text{B6})$$

$$\mathcal{C}^\theta(T_{1u} T_{1u}; H_g) = \frac{1}{4} \begin{pmatrix} -4 \sqrt{\frac{2}{3}} + 2 \sqrt{6} \sin^2 \theta & \sqrt{3} \sin 2\theta & -\sqrt{3} \sin 2\theta \\ \sqrt{3} \sin 2\theta & 2\sqrt{\frac{2}{3}} - \sqrt{6} \sin^2 \theta & \sqrt{6} \sin^2 \theta \\ -\sqrt{3} \sin 2\theta & \sqrt{6} \sin^2 \theta & 2\sqrt{\frac{2}{3}} - \sqrt{6} \sin^2 \theta \end{pmatrix}. \quad (\text{B7})$$

The eigenvalues of these two matrices are independent of θ and given by $(0, -\frac{1}{\sqrt{2}}, \frac{1}{\sqrt{2}})$ and $(-\frac{2}{\sqrt{6}}, \frac{1}{\sqrt{6}}, \frac{1}{\sqrt{6}})$ which implies that the splitting is independent of the orientation of the molecule with respect to the direction of the applied $l = 1$ and $l = 2$ potentials. The coupling of the HOMO (H_u) to the lower lying H_g and G_g levels is given by

$$\mathcal{C}^\theta(H_u H_g; T_{1u}) = \frac{1}{2\sqrt{5}} \begin{pmatrix} 0 & \sqrt{3} \sin \theta & -\sqrt{3} \sin \theta & 0 & 0 \\ \sqrt{3} \sin \theta & -\sqrt{2} \cos \theta & 0 & \sqrt{2} \sin \theta & 0 \\ -\sqrt{3} \sin \theta & 0 & \sqrt{2} \cos \theta & 0 & -\sqrt{2} \sin \theta \\ 0 & \sqrt{2} \sin \theta & 0 & -2\sqrt{2} \cos \theta & 0 \\ 0 & 0 & -\sqrt{2} \sin \theta & 0 & 2\sqrt{2} \cos \theta \end{pmatrix}, \quad (\text{B8})$$

$$\mathcal{C}^\theta(H_u G_g; T_{1u}) = \frac{1}{2\sqrt{5}} \begin{pmatrix} \sqrt{3} \sin \theta & 2\sqrt{2} \cos \theta & 0 & -\frac{1}{\sqrt{2}} \sin \theta & 0 \\ -\sqrt{3} \sin \theta & 0 & -2\sqrt{2} \cos \theta & 0 & \frac{1}{\sqrt{2}} \sin \theta \\ 0 & -\sqrt{2} \sin \theta & 0 & -\sqrt{2} \cos \theta & -\frac{3}{\sqrt{2}} \sin \theta \\ 0 & 0 & \sqrt{2} \sin \theta & \frac{3}{\sqrt{2}} \sin \theta & \sqrt{2} \cos \theta \end{pmatrix}. \quad (\text{B9})$$

The coupling of the HOMO among themselves is given by

$$\mathcal{C}^\theta(1; H_u H_u; H_g) = \frac{1}{4\sqrt{5}} \begin{pmatrix} -8 + 12 \sin^2 \theta & \sqrt{\frac{3}{2}} \sin 2\theta & \sqrt{\frac{3}{2}} \sin 2\theta & \sqrt{\frac{3}{2}} \sin^2 \theta & \sqrt{\frac{3}{2}} \sin^2 \theta \\ \sqrt{\frac{3}{2}} \sin 2\theta & 2 - 3 \sin^2 \theta & -3 \sin^2 \theta & -3 \sin 2\theta & 3 \sin^2 \theta \\ \sqrt{\frac{3}{2}} \sin 2\theta & -3 \sin^2 \theta & 2 - 3 \sin^2 \theta & 3 \sin^2 \theta & -3 \sin 2\theta \\ \sqrt{\frac{3}{2}} \sin^2 \theta & -3 \sin 2\theta & 3 \sin^2 \theta & 2 - 3 \sin^2 \theta & 3 \sin 2\theta \\ \sqrt{\frac{3}{2}} \sin^2 \theta & 3 \sin^2 \theta & -3 \sin 2\theta & 3 \sin 2\theta & 2 - 3 \sin^2 \theta \end{pmatrix}, \quad (\text{B10})$$

$$\mathcal{C}^\theta(2; H_u H_u; H_g) = \frac{1}{4} \begin{pmatrix} 0 & \sqrt{\frac{3}{2}} \sin 2\theta & \sqrt{\frac{3}{2}} \sin 2\theta & -\sqrt{\frac{3}{2}} \sin^2 \theta & -\sqrt{\frac{3}{2}} \sin^2 \theta \\ \sqrt{\frac{3}{2}} \sin 2\theta & 2 - 3 \sin^2 \theta & \sin^2 \theta & \sin 2\theta & \sin^2 \theta \\ \sqrt{\frac{3}{2}} \sin 2\theta & \sin^2 \theta & 2 - 3 \sin^2 \theta & \sin^2 \theta & \sin 2\theta \\ -\sqrt{\frac{3}{2}} \sin^2 \theta & \sin 2\theta & \sin^2 \theta & -2 + 3 \sin^2 \theta & \sin 2\theta \\ -\sqrt{\frac{3}{2}} \sin^2 \theta & \sin^2 \theta & \sin 2\theta & \sin 2\theta & -2 + 3 \sin^2 \theta \end{pmatrix}. \quad (\text{B11})$$

In equation (B5) the product $\mathcal{C}^\theta(xx'; T_{1u})^\top \mathcal{C}^\theta(xx'; T_{1u})$ enters. For the matrices given in (B6), (B8) and (B9) these products can be expressed in terms of the $l = 2$ coupling matrices (B7), (B10) and (B11):

$$\mathcal{C}^\theta(T_{1u}T_{1g}; T_{1u})^\top \mathcal{C}^\theta(T_{1u}T_{1g}; T_{1u}) = \frac{1}{3} + \frac{1}{\sqrt{6}} \mathcal{C}^\theta(T_{1u}T_{1u}; H_g), \quad (\text{B12})$$

$$\mathcal{C}^\theta(H_u H_g; T_{1u})^\top \mathcal{C}^\theta(H_u H_g; T_{1u}) = \frac{1}{5} + \frac{\sqrt{5}}{10} \mathcal{C}^\theta(1; H_u H_u; H_g) - \frac{3}{10} \mathcal{C}^\theta(2; H_u H_u; H_g), \quad (\text{B13})$$

$$\mathcal{C}^\theta(H_u G_g; T_{1u})^\top \mathcal{C}^\theta(H_u G_g; T_{1u}) = \frac{1}{5} + \frac{\sqrt{5}}{10} \mathcal{C}^\theta(1; H_u H_u; H_g) + \frac{3}{10} \mathcal{C}^\theta(2; H_u H_u; H_g). \quad (\text{B14})$$

Using these relations, the total coupling matrix (neglecting the constant terms in the previous relations) due to the applied $l = 1$ and $l = 2$ potential, is given by

$$H'(T_{1u}, \theta) = \left(V_{10}^2 c_1 + V_{20} c_2 \right) \mathcal{C}^\theta(T_{1u}T_{1u}; H_g), \quad (\text{B15})$$

$$H'(H_u, \theta) = V_{10}^2 d_1 \left[\cos \delta_1 \mathcal{C}^\theta(1; H_u H_u; H_g) + \sin \delta_1 \mathcal{C}^\theta(2; H_u H_u; H_g) \right] + \quad (\text{B16})$$

$$V_{20} d_2 \left[\cos \delta_2 \mathcal{C}^\theta(1; H_u H_u; H_g) + \sin \delta_2 \mathcal{C}^\theta(2; H_u H_u; H_g) \right], \quad (\text{B17})$$

where $c_1 = \frac{1}{\sqrt{6}} \frac{t(T_{1u}T_{1g}; T_{1u})^2}{E_{T_{1u}} - E_{T_{1g}}}$ and $c_2 = t(T_{1u}T_{1u}; H_g)$. Similarly we have $d_1 \cos \delta_1 = \frac{\sqrt{5}}{10} \left[\frac{t(H_u H_g; T_{1u})^2}{E_{H_u} - E_{H_g}} + \frac{t(H_u G_g; T_{1u})^2}{E_{H_u} - E_{G_g}} \right]$, $d_1 \sin \delta_1 = \frac{3}{10} \left[-\frac{t(H_u H_g; T_{1u})^2}{E_{H_u} - E_{H_g}} + \frac{t(H_u G_g; T_{1u})^2}{E_{H_u} - E_{G_g}} \right]$ and $d_2 \cos \delta_2 = t_1(H_u H_u; H_g)$, $d_2 \sin \delta_2 = t_2(H_u H_u; H_g)$. Equation (B15) implies that the contributions of the $l = 1$ and $l = 2$ to the splitting of the LUMO add up trivially. Using the values in table III and the energies of figure 3 yields the values $\delta_1 = 0.064$ and $\delta_2 = 0.037$, which are almost equal when compared to π . This can be understood by the following remarks: $\delta_1 = 0$ in the case of $t(H_u H_g; T_{1u}) = t(H_u G_g; T_{1u})$ and $E_{H_g} = E_{G_g}$. Furthermore, it can be shown that $\delta_2 = \arctan(1/\sqrt{125}) \approx 0.090$ assuming that the angular dependence of the HOMO is given by $l = 5$ spherical harmonics. Taking an average value of $\delta = 0.050$ yields the approximate relation

$$H'(H_u, \theta) \approx \left(V_{10}^2 d_1 + V_{20} d_2 \right) \left[\cos \delta \mathcal{C}^\theta(1; H_u H_u; H_g) + \sin \delta \mathcal{C}^\theta(2; H_u H_u; H_g) \right], \quad (\text{B18})$$

which shows that, to a good approximation, the contributions of the $l = 1$ and $l = 2$ potential to the splitting of the HOMO add up trivially.

APPENDIX C: CALCULATION OF THE MATRIX β

In this section it is shown how to calculate the matrix β appearing in equation (16). The second term on the right side of this equation describes the coefficients of the term $\sum_{\mathbf{R}_i \neq 0} V^i(\mathbf{r} - \mathbf{R}_i)$ which enters the screened potential V^{scr} and which describes the potential induced by all neighboring sites. Using the definition (1), we can rewrite this expression as

$$\sum_{\mathbf{R}_i \neq 0} V^i(\mathbf{r} - \mathbf{R}_i) = \sum_{lm} Q_{lm} \sum_{\mathbf{R}_i \neq 0} I_{lm}^*(\mathbf{r} - \mathbf{R}_i) = \sum_{lm} Q_{lm} \sum_{\mathbf{R}_i \neq 0} (-1)^m I_{l-m}(\mathbf{r} - \mathbf{R}_i). \quad (\text{C1})$$

The function $I_{lm}(\mathbf{r}_1 - \mathbf{r}_2)$ can be decomposed using the translation formula (for $r_1 < r_2$)

$$I_{LM}(\mathbf{r}_1 - \mathbf{r}_2) = \sum_{\substack{l_1, l_2=0 \\ l_2-l_1=L}}^{\infty} (-1)^{l_2} \sqrt{\frac{(2l_2+1)!}{(2L+1)!(2l_1)!}} \sum_{m_1, m_2} C_{l_1 m_1 l_2 m_2}^{LM} R_{l_1 m_1}(\mathbf{r}_1) I_{l_2 m_2}(\mathbf{r}_2), \quad (\text{C2})$$

where $C_{l_1 m_1 l_2 m_2}^{LM}$ denote the Clebsch-Gordan coefficients. This formula can be found in different forms in the literature, see for example Ref. 14,15. Substituting (C2) in the sum (C1) with $\mathbf{r}_1 = \mathbf{r}$ and $\mathbf{r}_2 = \mathbf{R}_i$ yields

$$\sum_{\mathbf{R}_i \neq 0} V^i(\mathbf{r} - \mathbf{R}_i) = \sum_{\substack{l_1 m_2 \\ l_2 m_2}} \beta_{l_1 m_1 l_2 m_2} Q_{l_2 m_2} R_{l_1 m_1}(\mathbf{r}), \quad (\text{C3})$$

where the matrix β is given by

$$\begin{aligned}\beta_{l_1 m_1 l_2 m_2} &= (-1)^{m_2+l_2} \sqrt{\frac{[2(l_1+l_2)]!}{(2l_1)!(2l_2)!}} C_{l_1 m_1 l_2 -m_2}^{l_1+l_2 m_1-m_2} \sum_{\mathbf{R}_i \neq 0} I_{l_1+l_2 m_1-m_2}(\mathbf{R}_i) \\ &= (-1)^{m_2+l_2} \sqrt{\frac{(l_1+l_2+m_1-m_2)!(l_1+l_2-m_1+m_2)!}{(l_1+m_1)!(l_1-m_1)!(l_2+m_2)!(l_2-m_2)!}} \sum_{\mathbf{R}_i \neq 0} I_{l_1+l_2 m_1-m_2}(\mathbf{R}_i)\end{aligned}\quad (\text{C4})$$

In the last equality in (C4) the explicit form of the Clebsch-Gordan coefficients was used¹⁴. One verifies, that the matrix β is complex conjugate under the exchange of all indices. The remaining sums over the lattice sites \mathbf{R}_i in (C4) are easily performed by computer.

* Electronic address: swehrli@itp.phys.ethz.ch

¹ M.R. Beasley (Chair), S. Datta, H. Kogelnik, H. Kroemer, D. Monroe: *Report of the Investigation Committee on the Possibility of Scientific Misconduct in the Work of Hendrik Schön and Coauthors*, Sept. 2002, www.lucent.com/news_events/pdf/researchreview.pdf or publish.aps.org/reports/.

² P. Ball, Nature **421**, 878 (2003); J.-O. Lee, G. Lietschnig, F. Wiertz, M. Struijk, R.A.J. Janssen, R. Egberink, D.N. Reinhoudt, P. Hadlev, and C. Dekker, Nano Lett. **3**, 113 (2003); C.R. Kagan, A. Afzali, R. Martel, L.M. Gignac, P.M. Solomon, A.G. Schrott, and B. Ek, Nano Lett. **3**, 119 (2003).

³ R.E. Dinnebier, O. Gunnarsson, H. Brumm, E. Koch, P.W. Stephens, A. Huq, and M. Jansen, Science **296**, 109 (2002); E. Koch and O. Gunnarsson, Phys. Rev. B **67**, 161402(R) (2003).

⁴ H. Kempa and P. Esquinazi, cond-mat/0304105.

⁵ S. Wehrli, D. Poilblanc, and T.M. Rice, Eur. Phys. J. B **23**, 345 (2001).

⁶ M.R. Pederson and K.A. Jackson, Phys. Rev. B **41**, 7453 (1990); K. Jackson and M.R. Pederson, Phys. Rev. B **42**, 3276 (1990); A.A. Quong, M.R. Pederson, and J.L. Feldman, Solid State Commun. **87**, 535 (1993).

⁷ D. Porezag and M.R. Pederson, Phys. Rev. A **60**, 2840 (1999).

⁸ J.P. Perdew, K. Burke, and M. Ernzerhof, Phys. Rev. Lett. **77**, 3865 (1996).

⁹ M.R. Pederson and A.A. Quong, Phys. Rev. B **46**, 13584 (1992).

¹⁰ A.J. Stone, *The Theory of Intermolecular Forces* (Clarendon Press, Oxford, 1996).

¹¹ A. Auerbach, N. Manini, E. Tosatti, Phys. Rev. B **49**, 12998 (1994); N. Manini, E. Tosatti, A. Auerbach, Phys. Rev. B **49**, 13008 (1994);

¹² P.H. Butler, *Point Group Symmetry Applications* (Plenum Press, 1981).

¹³ M.S. Dresselhaus, G. Dresselhaus, and P.C. Eklund, *Science of Fullerenes and Carbon Nanotubes* (Academic Press, 1996).

¹⁴ D.A. Varshalovich, A.N. Moskalev, and V.K. Khersonskii, *Quantum Theory of Angular Momentum* (World Scientific, 1988).

¹⁵ M.A. Epton and B. Dembart, SIAM J. Sci. Comp. **16**, 865 (1994).

¹⁶ S. Baroni and S. de Gironcoli and A. Dal Corso., Rev. Mod. Phys. **73**, 515 (2001).

¹⁷ S. Wehrli, D. Poilblanc, T.M. Rice, M. Sigrist, published in: H. Kuzmany, J. Fink, M. Mehring, and S. Roth (Eds.): *Structural and Electronic Properties of Molecular Nanostructures*, AIP Conference Proceedings **633**, 213 (2002).

¹⁸ S. Satpathy, V. P. Antropov, O.K. Andersen, O. Jepsen, O. Gunnarsson, and A.I. Liechtenstein, Phys. Rev. B **46**, 1773 (1992); N. Laouini, O.K. Andersen, and O. Gunnarsson, Phys. Rev. B **51**, 17446 (1995).

¹⁹ O. Gunnarsson, S. Satpathy, O. Jepsen, and O.K. Andersen, Phys. Rev. Lett. **67**, 3002 (1991).

²⁰ P.A. Brühwiler, A.J. Maxwell, P. Baltzer, S. Andersson, D. Arvanitis, L. Karlsson, and N. Mårtensson, Chem. Phys. Lett. **279**, 85 (1997).

²¹ N. Manini, G.E. Santoro, A. Dal Corso, and E. Tosatti, Phys. Rev. B **66**, 115107 (2002).

²² O. Gunnarsson, E. Koch, and R.M. Martin, Phys. Rev. B **54**, 11026 (1996); E. Koch, O. Gunnarsson, and R.M. Martin, Phys. Rev. B **60**, 15714 (1999).

²³ E. Koch, O. Gunnarsson, S. Wehrli, and M. Sigrist, to be published in: H. Kuzmany, J. Fink, M. Mehring, and S. Roth (Eds.): *Electronic Properties of Novel Materials*, American Institute of Physics, 2003.